Supporting Information

Elhai et al. 10.1073/pnas.1523512113

SI Materials and Methods

Serum Levels of OX40L. All patients fulfilled the 2013 European League Against Rheumatism/American College of Rheumatology (EULAR/ACR) classification criteria for SSc (39). Among the patients with SSc, 147 (83.1%) were female and 30 were men. The mean age (± SD) of patients with SSc was 56.9 ± 13.8 y. The mean disease duration was 9.8 ± 8.2 y; 70/171 (41%) patients had the diffuse cutaneous subset, and 101 (59%) had the limited form according to Leroy's criteria (40). Pulmonary hypertension was defined by precapillary pulmonary hypertension on right heart catheterization (resting mean pulmonary artery pressure ≥25 mmHg together with a pulmonary capillary wedge pressure of ≤15 mmHg) (41). Fibrosing alveolitis was searched by high-resolution CT (HRCT). Among these patients, 124 were followed up for a mean 5.6 ± 2.9 y. A high level of serum OX40L at baseline was considered to be a serum OX40L level higher or equal to that in the 95% percentile of healthy patients, i.e., 8.4370 ng/mL. Progression of dermal fibrosis was defined by worsening of Rodnan skin score by ≥10% and was observed in 14/103 (13.6%) patients with SSc during the follow-up period (42). Worsening of fibrosing alveolitis was defined by new-onset lung fibrosis on HRCT and/or deterioration of lung volume (≥10% of forced vital capacity) during the follow-up period. Progression of fibrosing alveolitis was observed in 28/122 (22.9%) patients with SSc.

The replication study cohort was derived from the ongoing, prospective, observational Oslo University Hospital SSc cohort study and included all cases that met the 2013 EULAR/ACR classification criteria for SSc and for which longitudinal clinical data were available (31, 43). Paired pulmonary function tests (PFTs) and HRCT lung images were obtained at baseline and at the last available follow-up visit, and the extent of fibrosis measured precisely, as previously described (31).

The SSc study cohort included 241 patients. Mean age at disease onset was 48 y (SD 15.4), the mean follow-up period was 3.9 y (SD 2.9), and mean disease duration was 5.9 y (SD 6.1). The baseline PFT and HRCT data were obtained a mean of 1.7 y before the serum used for the cross-sectional OX40L analyses was obtained; the corresponding follow-up data for the predictive model were from a mean of 2.8 y after serum sampling.

mAb Against OX40L. One hybridoma producing a neutralizing mAb against mouse OX40L (RM134L, rat IgG2b) was used as previously described (7–10). This hybridoma was grown in RPMI 1640 medium with FCS; then the supernatant was purified by protein G chromatography and was quantified using spectrophotometry. The purity of the obtained antibody was assessed by PAGE.

Animal Care. The animals were kept under standard laboratory conditions. Diet and water were provided ad libitum. Animal welfare was assessed every 2 d, and animals were weighed weekly.

Bleomycin-Induced Dermal Fibrosis in OX40L-Deficient Mice. OX40L-deficient mice were purchased from Jackson Laboratory. Mice on a C57BL/6 background expressing OX40L ($ox40l^{+/+}$) were purchased from Janvier. Skin fibrosis was induced in 6-wk-old male mice by local injections of bleomycin for 3 wk; 100 μL of bleomycin dissolved in 0.9% NaCl at a concentration of 0.5 mg/mL was administered every other day by s.c. injection in defined 1-cm^2 areas of the upper back (32). Injections of 0.9% NaCl (100 μL s.c.) were used as controls. Four different groups, consisting of two groups of $ox40l^{-/-}$ mice and two groups of $ox40l^{+/+}$ mice were analyzed. One group of $ox40l^{-/-}$ mice and one group of $ox40l^{+/+}$ mice were challenged with bleomycin; the other two groups were injected with NaCl. The four groups consisted of 30 mice in total.

Prevention and Treatment of Bleomycin-Induced Fibrosis with Anti-OX40L mAb. Skin fibrosis was induced in 6-wk-old, pathogen-free, male C57BL/6 mice (Janvier) by injection of bleomycin for 3 wk, as previously described. Injections (s.c.) of 100 μL 0.9% NaCl, the solvent for bleomycin, was used as controls. The weight of the mice was 20–25 g.

Collagen Measurements. The collagen content in lesional skin samples was explored by hydroxyproline assay, as previously described (33, 35). Briefly, each sample was hydrolyzed and titrated to a pH of 7. This solution was combined with chloramine T and p-dimethylaminobenzaldehyde in perchloric acid and was read at 557 nm with a spectrophotometer (Molecular Devices). Two samples from each mouse were analyzed in this experiment.

Immunohistochemistry for α-SMA, OX40L, c-Fos, c-Fun, CD3, CD22, CD57, and CD68. Myofibroblasts were identified by staining for α-SMA (33). Cells positive for α-SMA in mouse skin sections were detected by incubation with monoclonal anti–α-SMA antibody (clone 1A4; Sigma-Aldrich) at a dilution of 1:1,000 for 3 h at room temperature. Polyclonal rabbit anti-mouse labeled with HRP (Dako) was used as secondary antibody for 1 h at room temperature. The number of myofibroblasts was determined at 200× magnification in four different sections from each mouse by two blinded examiners (M.F. and M.E.). To quantify the numbers of infiltrating T cells, B cells, NK cells, and macrophages and the expression of c-fos and c-jun, lesional skin sections from $ox40l^{-/-}$ and $ox40l^{+/+}$ mice were incubated with polyclonal rabbit anti-mouse antibodies for CD3 (dilution 1:50), CD22 (dilution 1:100), or CD57 (1/200) or with polyclonal mouse anti-mouse antibodies for CD68 (dilution 1:100) or c-fos (dilution 1:100), or with monoclonal rabbit anti-mouse antibodies for c-jun (dilution 1:50) (all antibodies from Abcam) overnight at 4 °C, after antigen retrieval, as previously described (33, 35). Polyclonal goat anti-rabbit or rabbit anti-mouse (Dako) was used as the secondary antibody (dilution 1:200). T cells, B cells, and macrophages were counted in eight different sections of lesional skin of each mouse at 400× magnification. Counting was performed in a blinded manner by two examiners (M.F. and M.E.).

The expression of OX40L in lesional skin from patients with SSc and in skin from controls was detected by overnight staining at 4 °C with polyclonal rabbit anti-human OX40L antibody or isotype control at a dilution of 1:100 (Sigma-Aldrich). Polyclonal goat anti-rabbit antibody (Dako) was used as secondary antibody (dilution 1:200). The intensity of OX40L immunostaining was quantified with ImageJ software, as described at rsbweb.nih.gov/ij/docs/examples/stained-sections/index.html.

Immunofluorescence for OX40L, CD3, CD22, CD31, α-SMA, c-Fos, and CD90. For costaining experiments, immunofluorescent staining was performed in lesional skin from patients with SSc. The protocol and antibodies were similar to the immunohistochemistry protocol. Fibroblasts were identified by staining for polyclonal rabbit anti-human antibodies for CD90 (dilution 1:100) (Abcam). Alexa Fluor 594 goat anti-mouse IgG and Alexa Fluor 488 goat anti-rabbit antibodies (Life Technologies) were used as secondary antibodies for 1 h at room temperature at a dilution of 1:200. Slides were mounted on a coverslip with a drop of mounting

medium and were stored in the dark at +4 °C until analysis. OX40L expression also was assessed on SSc fibroblasts and healthy fibroblasts cultured in vitro. Nuclei were stained using DAPI.

For costaining between c-fos and CD3 and α-SMA, as well as CD31 (dilution 1:100) (Abcam) and α-SMA. Alexa Fluor 594 goat anti-rabbit IgG and Alexa Fluor 488 goat anti-rabbit antibodies (Life Technologies) were used as secondary antibodies. The intensity of α-SMA^{+} cells expressing c-fos was quantified with ImageJ software.

Inflammatory Cytokine Measurement in Lesional Skin Samples from Bleomycin-Treated Mice. Cytokine levels were measured in the skin of 16 ox40l$^{-/-}$ and ox40l$^{+/+}$ mice subjected to bleomycin or NaCl injections (four mice per group), as previously described (33, 35). Briefly, mouse skin tissue lysate was prepared by homogenization in modified RIPA buffer with a Precellys 24 tissue homogenizer/grinder (Ozyme). Skin lysates were assayed for the following cytokines by multiplex bead array technology (BD Biosciences): TNF-α, IL-6, IFN-γ, IL-4, IL-10, and IL-17.

Effects of OX40L Inhibition in the Tsk-1 Mouse Model. Five Tsk-1 mice (purchased from Jackson Laboratory) were treated with 300 μg anti-OX40L mAb, and four Tsk-1 mice were treated with control IgG three times/wk i.p., starting at age 5 wk (before the development of fibrosis). Another group consisted of five pa/pa (control) mice. The hypodermal thickness was determined by measuring the thickness of the s.c. connective tissue beneath the panniculus carnosus at four different sites on the upper back in each mouse at 40× magnification. The measurement was performed by two independent blinded investigators (M.P. and M.E.).

Microscopy. Images were captured with a Nikon Eclipse 80i microscope equipped with a DSP 3CCD camera (Sony) or with a Lamina multilabel slide scanner (PerkinElmer) or on a Zeiss Axio Observer Z1 microscope with dry 40× and dry 63× objectives and a CoolSNAP HQ2 CCD camera.

Prevention of Fibrosing Alveolitis and PAH in the Fra-2 Model. Fra-2 transgenic mice were obtained from a collaboration established with Sanofi Genzyme. Two groups of eight and seven Fra-2 transgenic mice, respectively, were treated by anti-OX40L mAb or control rat IgG, as previously described, starting when mice were 13 wk old, before the appearance of fibrosing alveolitis and vasculopathy. Two control groups of five C57/BL6 mice were treated by i.p. injections of anti-OX40L mAb and control rat IgG, respectively. Because results in the two control groups (i.e., C57/BL6 mice injected with anti-OX40L or with control IgG) were similar, these groups were analyzed together. Mice were killed by cervical dislocation at age 17 wk.

Expression of OX40 and OX40L by Fra-2 Transgenic Mice. Expression of OX40 and OX40L by Fra-2 transgenic mice was assessed in the skin and in the lungs of the mice by PCR (Taqman).

Assessment of Fibrosing Alveolitis by Micro-CT. For assessment of fibrosing alveolitis, the animals were placed in the supine position on the CT table. CT images were obtained with a PerkinElmer Quantum FX system (Caliper Life Sciences).

Mice were sedated with 3–4% isoflurane anesthesia (0.5–1.5 L/min) for induction via a nose cone. Anesthesia was maintained with 2.5–3% isoflurane (400–800 mL/min) during the acquisition. During image acquisition thoracic breathing movements were recorded, detecting the upward and downward movement of the thorax. Images were acquired throughout the spontaneous respiratory cycle. Only images acquired during expiration were analyzed. Images were acquired with the following parameters: 90 kV X-ray source voltage, 160 μA current. Total scanning time was ∼4.5 min per mouse. Tomograms were reconstructed using Rigaku software. The analysis began with the isolation of lung tissue by a manually drawn volume of interest. Analysis of lung density and drawing was performed with CTAn Bruker software. Lung density was measured in Hounsfield units (HU) after calibration. A phantom calibration was made on the acquisition Rigaku software: a water-filled 1.5-mL tube inside a 2-mL tube was scanned. Based on full-stack histograms of a manually delimited volume-of-interest containing only water or air, the mean grayscale index of water was set at 0 HU, and the grayscale index of air was set at −1,000 HU. This value was reported in the CTAn Bruker software.

Histopathologic Assessment of Fibrosing Alveolitis. The severity of fibrosing alveolitis was semiquantitatively assessed according to the method described by Ashcroft et al. (37) by two examiners blinded to the genotype and the treatment (O.A. and M.E.). Lung fibrosis was graded on a scale of 0–8 by examining randomly chosen fields of the left upper lobe. The grading criteria were as follows: grade 0: normal lung; grade 1: minimal fibrous thickening of alveolar walls; grade 3: moderate thickening of walls without obvious damage; grade 5: increased fibrosis with definite damage and formation of fibrous bands; grade 7: severe distortion of structure and large fibrous areas; and grade 8: total fibrous obliteration. Grades 2, 4, and 6 were used as intermediate stages between these criteria. All images were taken with a Lamina multilabel slide scanner.

Nonlinear Microscopy and SHG Processing. A multiphoton inverted-stand Leica SP5 microscope (Leica Microsystems GmbH) was used for tissue imaging. A Ti:Sapphire Chameleon Ultra laser (Coherent) with a center wavelength at 810 nm was used as the laser source for SHG and TPEF signals. The laser beam was circularly polarized to ensure isotropic excitation of the sample regardless of the orientation of fibrillar collagen. A Leica Microsystems HCX IRAPO 25×/0.95 W objective was used to excite and collect SHG and TPEF signals. Signals were detected in epi-collection through 405/15-nm and 525/50-nm bandpass filters, respectively, by non-descanned photomultiplier tube detectors (Leica Microsystems) with a constant voltage supply, at constant laser excitation power, allowing direct comparison of SHG intensity values. Two fixed thresholds were chosen to distinguish biological material from the background signal (TPEF images) and specific collagen fibers (SHG images). The SHG score was established by comparing the area occupied by the collagen relative to the sample surface. Image processing and analysis (thresholding and SHG scoring) were performed using ImageJ homemade routines (imagej.nih.gov/ij) as previously described (38). Results were normalized to control C57/BL6 mice.

Statistics. To analyze whether serum OX40L was predictive of dermal, pulmonary, or vascular worsening, a Cox proportional hazard model was performed and summarized as HR and 95% CI. The correlation between the lung fibrosis score and the data obtained at micro-CT was assessed by calculating the Spearman's coefficient of rank correlation (ρ) and 95% CI.

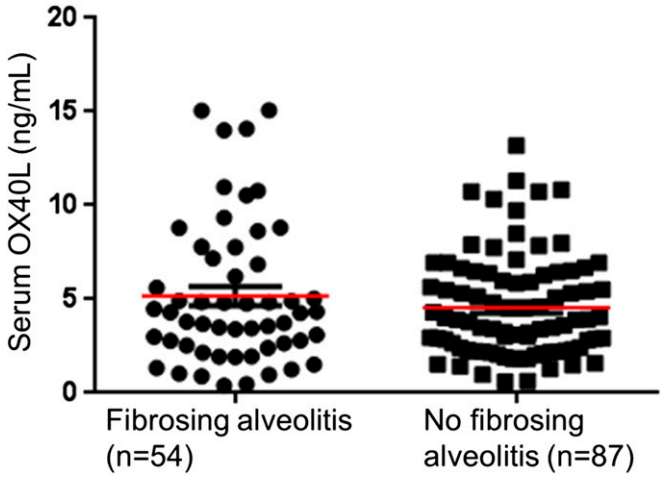

Fig. S1. Serum OX40L levels are not significantly different between SSc-patients with and without fibrosing alveolitis.

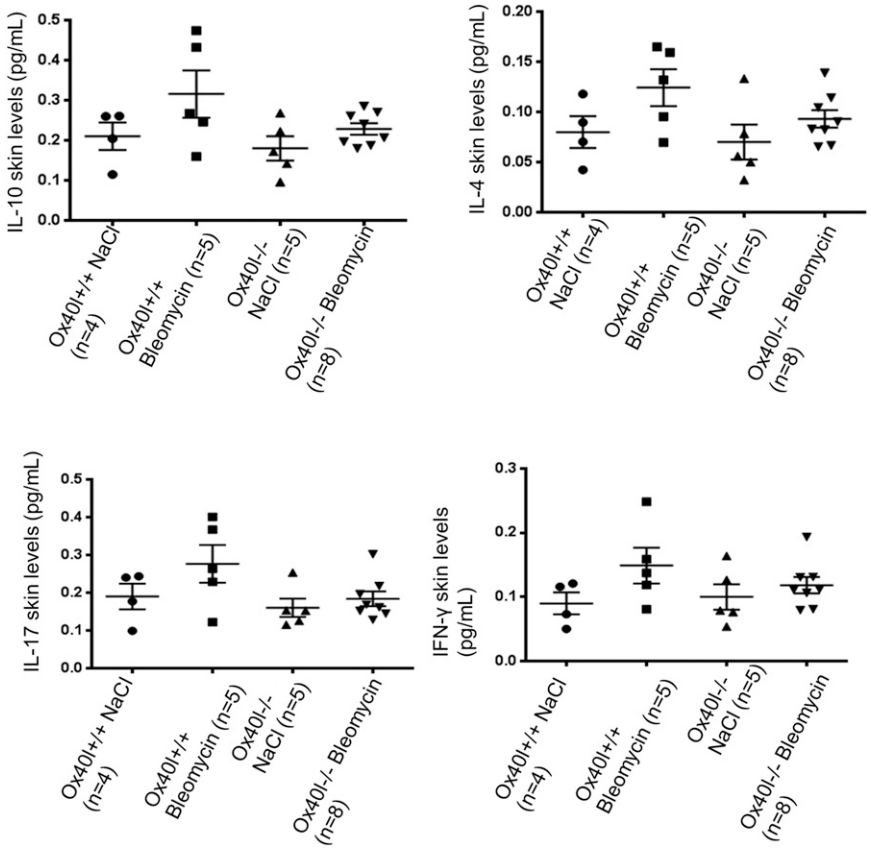

Fig. S2. Skin levels of the cytokines IL-10, IL-4, IL-17, and IFN-γ did not differ in ox40l$^{-/-}$ mice and ox40l$^{+/+}$ mice subjected to bleomycin. Twenty-two mice were used. All cytokine concentrations are normalized on total protein concentration.

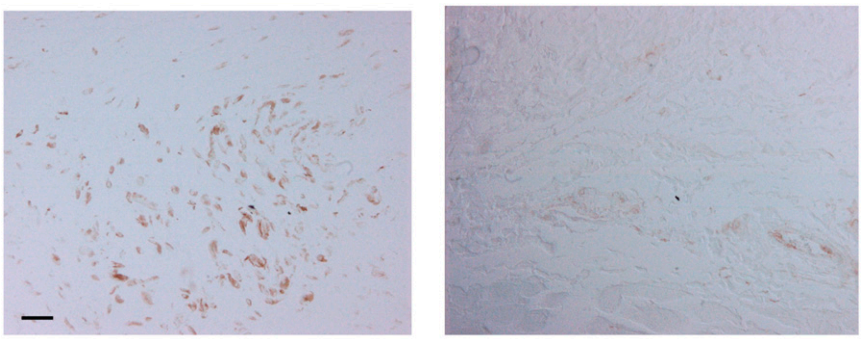

Fig. S3. Representative sections stained by immunohistochemistry for c-jun (magnification: 200×) from ox40l$^{+/+}$ and ox40l$^{-/-}$ mice receiving s.c. injections of bleomycin.

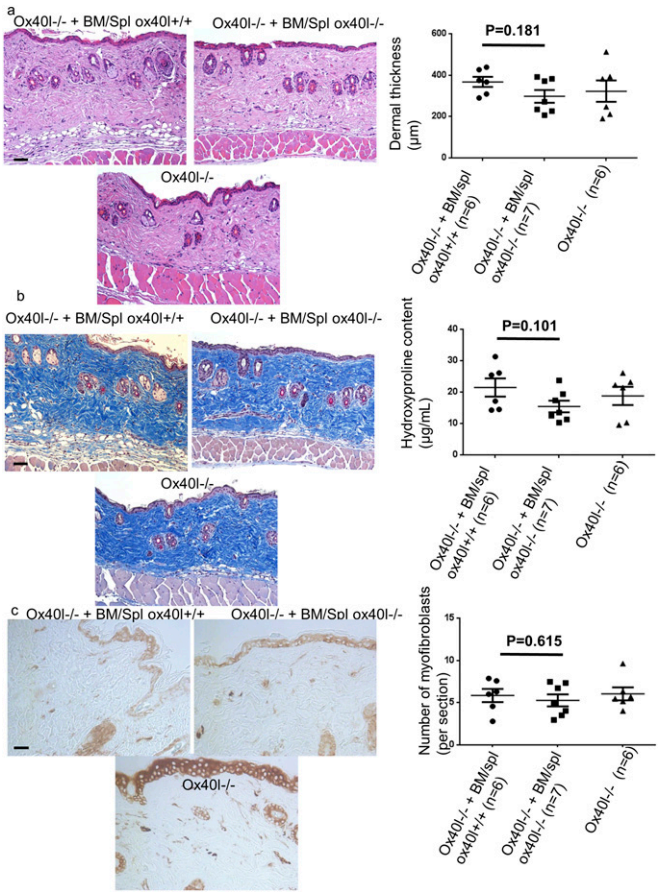

Fig. S4. Reconstitution of sublethally irradiated ox40l$^{-/-}$ mice with bone marrow and spleen cells from wild-type mice is not sufficient to reverse the protection of dermal fibrosis. (*A*) Representative H&E-stained sections (magnification: 100×) from sublethally irradiated ox40l$^{-/-}$ mice reconstituted with spleen and bone marrow cells from ox40l$^{+/+}$ mice (Ox40l$^{-/-}$ + BM/Spl ox40l$^{+/+}$) ($n = 7$), sublethally irradiated ox40l$^{-/-}$ mice reconstituted with spleen and bone marrow cells from ox40l$^{-/-}$ mice (Ox40l$^{-/-}$ + BM/Spl ox40l$^{-/-}$) ($n = 7$), and nonirradiated ox40l$^{-/-}$ mice ($n = 6$). All mice received s.c. injections of bleomycin ($n = 20$). One mouse from the Ox40l$^{-/-}$ + BM/Spl ox40l$^{+/+}$ group died. (Scale bar: 100 μm.) (*B*) Representative sections stained by trichrome. (Magnification: 100×.) (Scale bar: 100 μm.) There was a trend for increased hydroxyproline content in lesional skin of Ox40l$^{-/-}$ + BM/Spl ox40l$^{+/+}$ mice. (*C*) Myofibroblasts were identified by positive staining for α-SMA in slides. (Scale bar: 50 μm.) Values are represented by dot blots with the mean ± SEM; two-sided Mann–Whitney test.

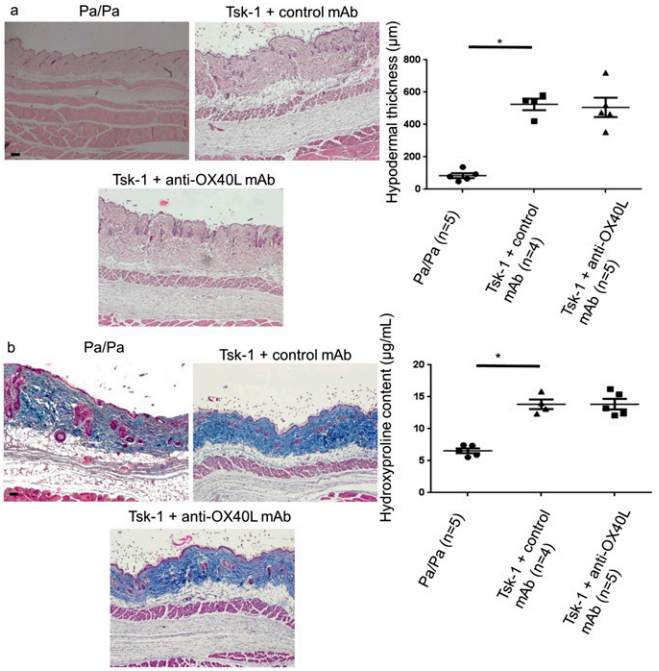

Fig. S5. OX40L inhibition has no effect in the Tsk-1 mouse model. (*A*) Representative H&E-stained sections (magnification: 40×) from control pa/pa mice ($n = 5$), Tsk-1 mice treated with control mAb ($n = 4$), and Tsk-1 mice treated with anti-OX40L mAb ($n = 5$). (Scale bar: 250 μm.) (*B*) Hydroxyproline content is not significantly different in Tsk-1 mice treated with anti-OX40L mAb or with control mAb. Representative samples stained by trichrome are shown. (Magnification: 40×.) Values are represented by dot blots with means ± SEM. Control mice were pa/pa mice. The experiment was performed in two independent series. *$P <$ 0.05; two-sided Mann–Whitney test.

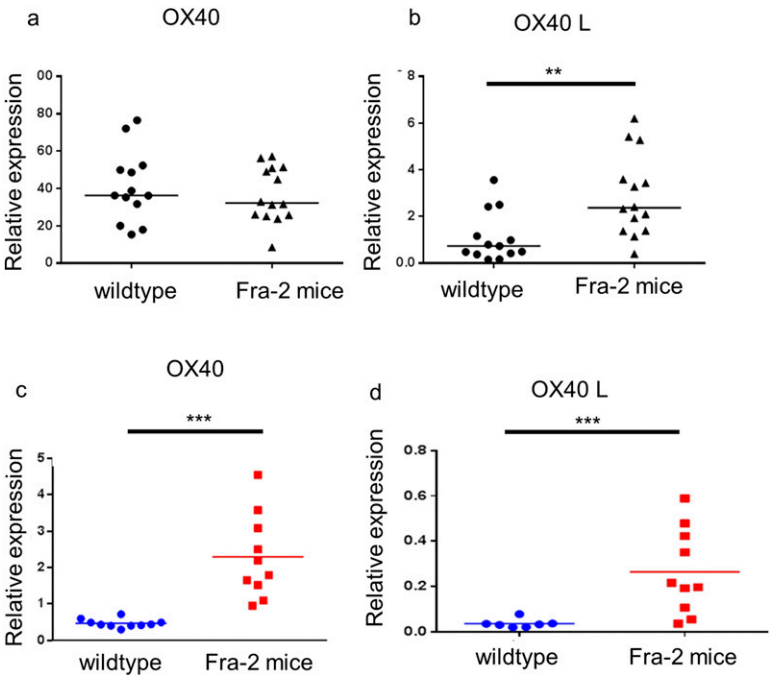

Fig. S6. OX40 and OX40L are overexpressed in skin and lungs of Fra-2 transgenic mice. (*A* and *B*) Expression of OX40 (*A*) and OX40L (*B*) was assessed in the skin of 14 Fra-2 mice and 10 wild-type control mice by quantitative PCR (Taqman). (*C* and *D*) OX40 (*C*) and OX40L (*D*) expression also was assessed in the lungs of 10 wild-type mice and 10 Fra-2 mice. **$P < 0.01$; ***$P < 0.001$.

Table S1. Association of extensive disease at follow-up, FVC% decline >5% and FVC <70% at follow-up, circulating Ox40L, and clinical parameters in the Oslo University Hospital SSc cohort (n = 241) in multivariable logistic regression

	FVC <70% at follow-up (range)	*P* value	Annual FVC decline >5% (range)	*P* value	Extensive lung disease* (range)	*P* value
OX40l	1.3 (1.01–1.80)	0.047	1.4 (1.06–1.79)	0.017	1.5 (1.03–2.31)	0.037
Anti-centromere Ab	NS	NS	NS	NS	NS	
dcSSc	4.1 (1.22–13.81)	0.027	NS	NS	NS	
Fibrosis at baseline	1.2 (1.09–1.22)	<0.001	NS	NS	1.3 (1.14–1.45)	<0.001
Age at disease onset	NS	NS	1.04 (1.01–1.07)	0.019	NS	NS

All values are adjusted for gender. Ab, antibody; dcSSc: diffuse cutaneous systemic sclerosis; FVC, forced vital capacity; NS, not significant.
*Defined by Goh and Wells (44) as >20% extent of interstitial lung disease (ILD) on HRCT and 10–30% extent of ILD and FVC <70%.